INTERNATIONAL JOURNAL FOR NUMERICAL METHODS IN FLUIDS, VOL. 22, 29–41 (1996)

PREDICTION OF AEROFOIL WAKE SUBJECTED TO THE EFFECTS OF CURVATURE AND PRESSURE GRADIENT

E. G. TULAPURKARA

Department of Aerospace Engineering, Indian Institute of Technology, Madras 600036, India

V. RAMJEE

Department of Applied Mechanics, Indian Institute of Technology, Madras 600036, India

AND

JACOB GEORGE

Department of Aerospace Engineering, Indian Institute of Technology, Madras 600036, India

SUMMARY

Experimental data on the development of wakes in a straight duct, a curved duct, a curved diffuser and a straight diffuser are compared with computations based on a finite volume scheme incorporating the k–ε model of turbulence. The results show that the computations based on the standard k–ε model are able to satisfactorily capture only the mean velocity profiles. To improve the predictions, several modifications to the model are tried out. Close agreement between experiment and computation as regards the velocity profiles, wake parameters and profiles of the turbulent kinetic energy k and Reynolds shear stress $\overline{u'v'}$ is obtained when modification to the model constant C_μ, based on the curvature parameter and the ratio of the production of turbulent kinetic energy to its rate of dissipation, is incorporated. The modified model is also able to capture the asymmetry in the profiles of k and $\overline{u'v'}$ caused by the curvature and its enhancement due to the additional presence of an adverse pressure gradient.

KEY WORDS: wake; curvature; pressure gradient; k–ε model of turbulence

1. INTRODUCTION

Thin shear flows with significant streamline curvature and pressure gradient are of considerable interest in many engineering applications. The field of turbomachinery provides many examples, such as flow over compressor and turbine blades. Another example is that of flow over a multielement aerofoil in which wake of the slat develops under the influence of both curvature and pressure gradient. An understanding of the turbulent structure in such flows is of basic importance and would help in improved prediction of the characteristics of aerofoils and turbine blades. Here we focus attention on the effects of curvature and pressure gradient on the development of wakes.

Many studies have been carried out to investigate the development of wakes with and without a pressure gradiant (see e.g. Reference 1–3). As regards the curvature effect on wakes, Savill[4] and Nakayama[5] have studied experimentally the development of wake in a curved flow. In these investigations the effects of curvature and pressure gradient were combined. To separate the two effects, Ramjee *et al.*[6] and Ramjee and Neelakandan[7] studied the development of wake in a curved duct of constant cross-section. In this manner the wake was subjected to the effect of curvature only. Narasimhan *et al.*[8] compared the experimental results of Ramjee and Neelakandan[7] with computations

CCC 0271–2091/96/010029–13

Received October 1994
Revised May 1995

based on the k–ε model of turbulence and found that the model was able to satisfactorily reproduce the mean velocity profiles. Further, the model was able to capture the asymmetry in the profiles of Reynolds shear stress, but the predicted peak values did not match the experimental values. Recently Tulapurkara *et al.*,[9] as a sequel to the work of Ramjee and Neelakandan,[7] studied the effect of the combination of curvature and pressure gradient on the wake of an aerofoil by allowing the wake to develop in a curved diffuser. They measured all the components of the Reynolds stresses. To separate the effects of curvature and pressure gradient, the development of wake was also studied in (a) a constant area straight duct, (b) a constant area curved duct and (c) a straight diffuser having the same pressure gradient as that in the curved diffuser.

In the present paper we examine whether this particular wake development[9] can be predicted by a numerical technique. The earlier experimental results[6,7] contain measurements of the Reynolds normal stresses $\overline{u'^2}$, $\overline{v'^2}$ and Reynolds shear stress $\overline{u'v'}$ only. Consequently, the values of the turbulent kinetic energy k calculated by Narasimhan *et al.*[8] could not be compared with the experimental data. In the present case, since all the Reynolds stresses have been measured, it is possible to compare the prediction of the turbulent kinetic energy also and examine the performance of the k–ε model in all its aspects. A brief description of the experimental work is given in the next section. This is followed by the details of the computational technique and the results.

2. EXPERIMENTAL RESULTS

The set-up is similar to that of Ramjee and Neelakandan[7] and is shown in Figure 1(a). It consists of a blower driven by a 2 hp motor. The blower is connected to a diffuser and then to a settling chamber. Two nylon screens and a honeycomb are provided in the settling chamber. The test section has a cross-section of 140×140 mm^2 and is 600 mm long. It is followed by either a straight duct, a curved duct, a curved diffuser or a straight diffuser depending on the case under investigation. The four cases under investigation are wake developing in (i) a straight duct of cross-section 140×140 mm^2 and 600 mm long, (ii) a curved duct of constant cross-sectional area 140×140 mm^2 and centreline radius $R = 700$ mm, (iii) a curved diffuser having an inlet cross-sectional area of 140×140 mm^2, an area ratio between exit and entry of 1·74, centreline radius $R = 700$ mm and turning angle $\beta = 60°$ and (iv) a straight diffuser having an area ratio of 1·54 and 600 mm long. The design of the curved diffuser is based on the guidelines provided by Fox and Kline.[10] In case (i), hereinafter denoted Flow A, the wake develops without curvature and pressure gradient effects. In case (ii), denoted Flow B, only the effect of streamline curvature is present. In case (iii), denoted Flow C, the wake is subjected to both streamline curvature and streamwise pressure gradient. In case (iv), denoted Flow D, only streamwise pressure gradient is present; the angle of divergence of the straight diffuser was adjusted to give almost the same centreline velocity as in the curved diffuser.

The velocity in the test section is about 15 m s^{-1}. The wake is produced by an NACA 0012 aerofoil of chord $c = 100$ mm kept at 0° incidence. The trailing edge is located 100 mm ahead of the exit to the test section. Figures 2(a)–2(d) show the variation in mean velocity U/U_{ref} for the wake in the four cases at $x = 150$, 200, 300 and 400 mm (i.e. $x/c = 1{\cdot}5$, 2, 3 and 4 respectively), where x is the distance from the trailing edge of the aerofoil along the centreline of the duct/diffuser. This range of x/c is likely to be sufficient for practical purposes. For example, in the case of a multielement aerofoil the length of the main wing chord is generally four times the chord of the slat. Thus the distance over which the wake of the slat is affected by the streamline curvature and pressure gradient effects caused by the presence of the main wing is about four times the chord of the wake-producing body. The quantity U_{ref} is the reference velocity measured in the test section at one chord length ahead of the aerofoil leading edge. The symbols W_{cd} and W_{sd} in the figures denote the width at the measuring

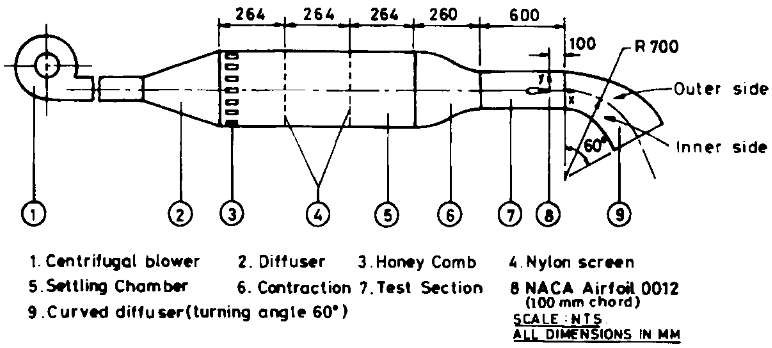

Figure 1(a). Experimental set-up

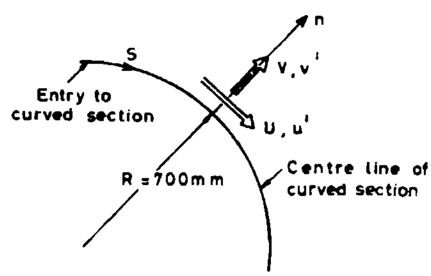

Figure 1(b). The (s, n) co-ordinate system

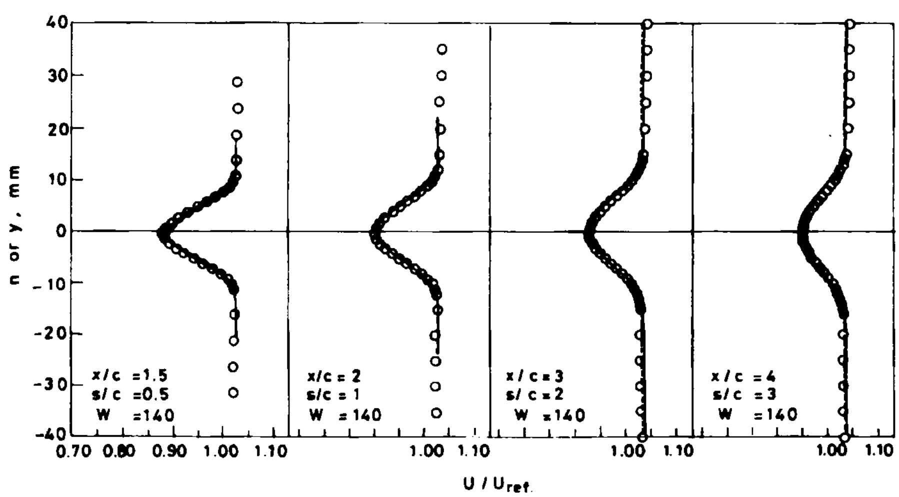

Figure 2(a). Mean velocity profiles (U/U_{ref})—Flow A: ○, experiment; ————, prediction with C_μ constant; --------, prediction with C_μ variable (Humphrey and Pourahmadi)

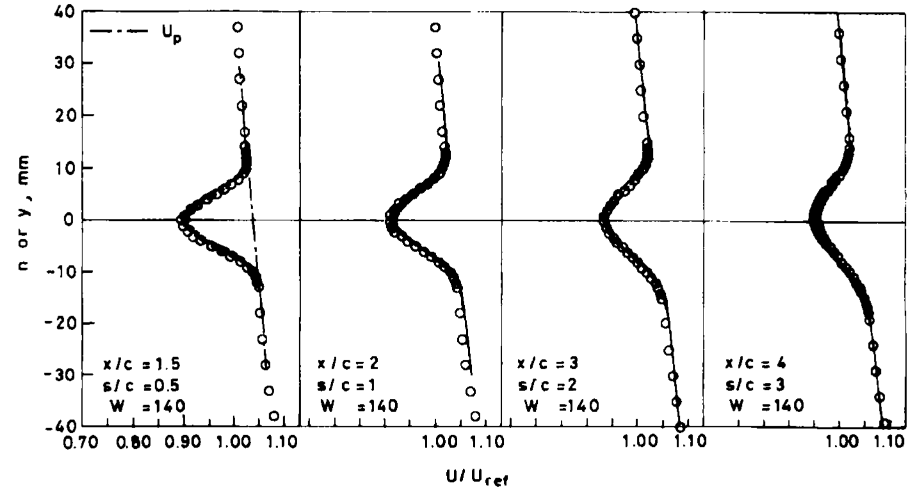

Figure 2(b). Mean velocity profiles (U/U_{ref})—Flow B: ○, experiment; ————, prediction with C_μ constant; — — —, prediction with C_μ variable (Leschziner and Rodi); --------, prediction with C_μ variable (Humphrey and Pourahmadi)

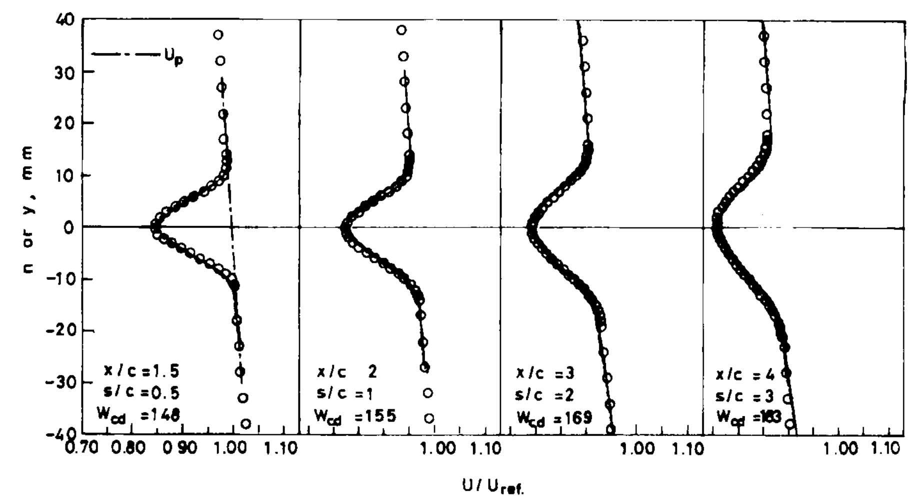

Figure 2(c). Mean velocity profiles (U/U_{ref})—Flow C: ○, experiment; ————, prediction with C_μ constant; — — —, prediction with C_μ variable (Leschziner and Rodi); --------, prediction with C_μ variable (Humphrey and Pourahmadi)

stations in the curved and straight diffusers respectively, while W in the figures denotes the width of the straight and curved ducts, which is 140 mm. The ordinate y is normal to the centreline of the duct.

The velocity distribution without the wake-producing body in Flows B and C was measured and is given by a line joining the velocity distribution outside the wake and the boundary layers on the walls. This is indicated by a chain line in Figure 2(b) and 2(c). This velocity is called U_p, the potential velocity. In the case of the wake developing in the curved diffuser (Flow C), the centreline velocity without the body, U_{pc}, is 15·00, 14·51, 13·86 and 13·17 m s^{-1} at $x/c = 1{\cdot}5$, 2, 3 and 4 respectively. This indicates that the average pressure gradient $d(U_{pc})/dx$ is $-7{\cdot}32$ s^{-1}. Almost the same value of pressure gradient was obtained by adjusting the divergence angle in Flow D. In Flows B and C, owing to the effect of curvature, the irrotational flow velocity outside the wake and the wall boundary layers is

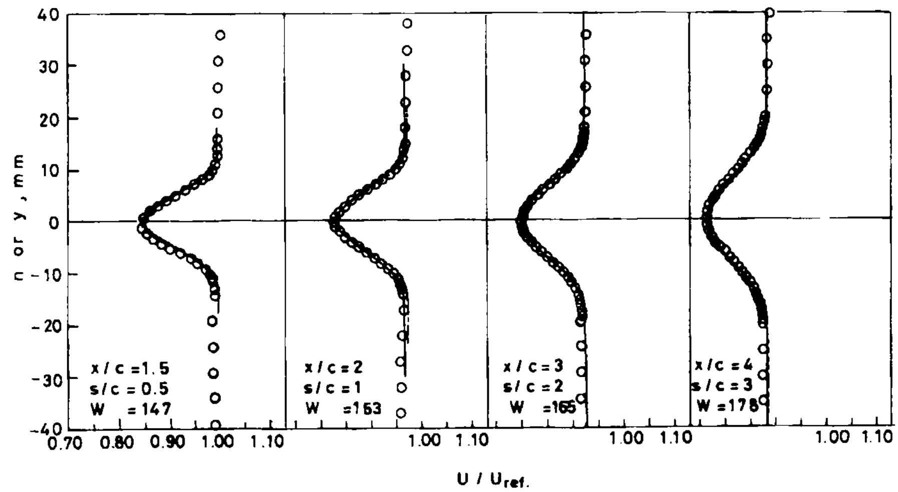

Figure 2(d). Mean velocity profiles (U/U_{ref})—Flow D: ○, experiment; ———, prediction with C_μ constant; — — —, prediction with C_μ variable (Leschziner and Rodi); --------, prediction with C_μ variable (Humphrey and Pourahmadi)

not constant over the cross-section. It is higher on the inner side than on the outer side. It may be mentioned that the inner side is the region between the wall, closer to the centre of the curvature, and the centreline while the outer side is between the centreline and the other wall (Figure 1(a)). A similar velocity profile was also observed by Nakayama.[5]

For the wake in the curved duct and diffuser the velocity defect W is obtained by subtracting U from U_p i.e. $W = U_p - U$. It is seen in Figures 2(b) and 2(c) that the velocity profile is asymmetric and the maximum velocity defect occurs near the centreline. Let the half-width b' be the value of y at which the velocity defect equals half of its maximum value. It is noticed that b' in Flows B and C is not the same on the two sides of the wake centreline as in Flows A and D. The variation in the maximum velocity defect W_0, non-dimensionalized by U_p, is shown in Figure 3. The variation in the average of the two half-widths, b'_{avg}, is shown in Figure 4. From the measured value of Reynolds stresses[9] the turbulent kinetic energy k was calculated. The profiles of the turbulent kinetic energy k/U_{ref}^2 for all the cases are shown in Figures 5(a)–5(d). For Flows A and D the turbulent kinetic energy profiles are symmetric about the wake centreline. For Flow B, owing to the effect of curvature, the values are higher on the inner side than on the outer side. This makes the profiles asymmetric. The profiles become further asymmetric when pressure gradient is present in addition to curvature (Flow C). The variations in the Reynolds shear stresses $\overline{u'v'}/U_{ref}^2$ for all the cases are shown in Figures 6(a)–6(d). The shear stress profiles are antisymmetric about the wake centreline in Flows A and D. The profiles are asymmetric when curvature is present (Flow B), with the asymmetry increasing with increase in x. This asymmetry is further enhanced in Flow C owing to the additional presence of adverse pressure gradient. Prediction of this behaviour is an important test for the model of turbulence and is one of the aims of the current investigation.

3. COMPUTATIONAL TECHNIQUE

The wakes in Flows A and D develop in a straight duct and a straight diffuser respectively and are computed using the scheme given by Badrinarayanan *et al.*[11] Flow B is computed using the scheme

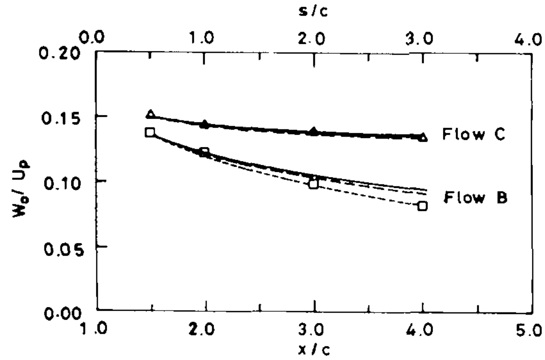

Figure 3. Streamwise variation in maximum velocity defect, W_0/U_p: □, △, experiment; ————, prediction with C_μ constant; — — —, prediction with C_μ variable (Leschziner and Rodi); ---------, prediction with C_μ variable (Humphrey and Pourahmadi)

developed by Narasimhan *et al.*[8] to compute the wake in a curved duct. This scheme is modified to compute the wake in Flow C. An outline of the scheme is as follows.

The thin shear flow equations for curved flows in an (s, n) co-ordinate system (Figure 1(b)) and incorporating the k–ε model of turbulence can be written as[12]

$$\partial U/\partial s + (\partial/\partial n)[(1 + n/R)V] = 0, \tag{1}$$

$$U\partial U/\partial s + V(1 + n/R)\partial U/\partial n = -UV/R - (1/\rho)\partial p/\partial s - 2\overline{u'v'}/R + (1 + n/R)\partial\overline{u'v'}/\partial n, \tag{2}$$

$$\begin{aligned} U\partial k/\partial s + V(1 + n/R)\partial k/\partial n = {} & (1 + n/R)\{\nu_t[\partial U/\partial n - (U/R)/(1 + n/R)]^2 - \varepsilon\} \\ & + (\partial/\partial n)[(\nu_t/\sigma_k)(1 + n/R)\partial k/\partial n], \end{aligned} \tag{3}$$

$$\begin{aligned} U\partial\varepsilon/\partial s + V(1 + n/R)\partial\varepsilon/\partial n = {} & (1 + n/R)\{C_{\varepsilon 1}\nu_t(\varepsilon/k)[\partial U/\partial n - (U/R)/(1 + n/R)]^2 \\ & - C_{\varepsilon 2}\varepsilon^2/k\} + (\partial/\partial n)[(\nu_t/\sigma_\varepsilon)(1 + n/R)\partial\varepsilon/\partial n], \end{aligned} \tag{4}$$

where the shear stress $\overline{u'v'} = \nu_t[\partial U/\partial n - (U/R)/(1 + n/R)]$, the eddy viscosity ν_t is given by $\nu_t = C_\mu k^2/\varepsilon$, $C_\mu = 0{\cdot}09$, $\sigma_k = 1{\cdot}0$, $C_{\varepsilon 1} = 1{\cdot}44$, $C_{\varepsilon 2} = 1{\cdot}92$, $\sigma_\varepsilon = 1{\cdot}3$, U and V are the mean velocities in the s- and n-direction (Figure 1(b)) respectively, u' and v' are the fluctuating velocity components of U and V respectively, k is the turbulent kinetic energy and ε is the rate of dissipation of

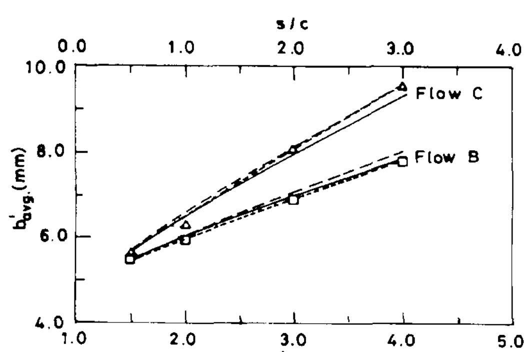

Figure 4. Streamwise variation in wake average half-width, b'_{avg}: □, △, experiment; ————, prediction with C_μ constant; — — —, prediction with C_μ variable (Leschziner and Rodi); ---------, prediction with C_μ variable (Humphrey and Pourahmadi)

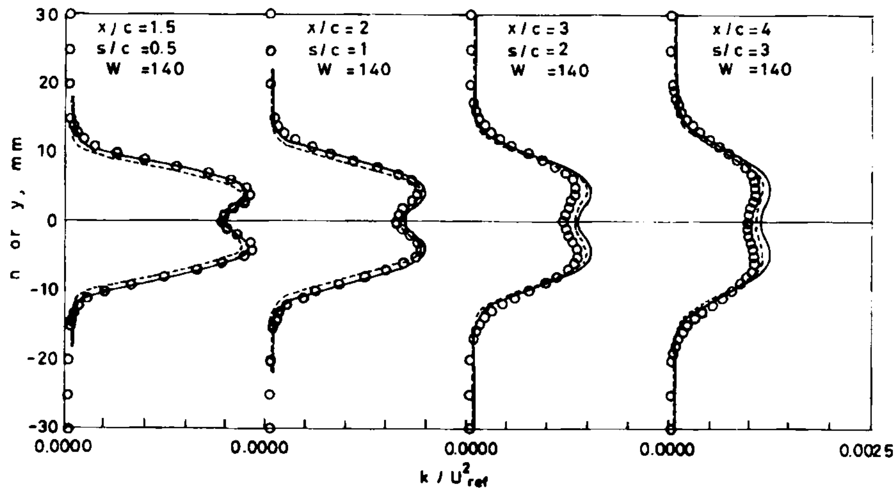

Figure 5(a). Profiles of turbulent kinetic energy, k/U_{ref}^2— Flow A: ○, experiment; ———, prediction with C_μ constant; --------, prediction with C_μ variable (Humphrey and Pourahmadi)

k. The s-co-ordinate line coincides with the centreline of the curved duct/diffuser and n is normal to it. C_μ, σ_k, $C_{\varepsilon 1}$, $C_{\varepsilon 2}$ and σ_ε are the constants in the standard k–ε model.

To reduce the above equations to a parabolic set, the gradient of pressure in the streamwise direction, $\partial p/\partial s$, needs to be prescribed. In a straight wake there is no cross-stream pressure gradient and $\partial p/\partial s$, which is constant across the wake, is obtained by applying Bernoulli's equation to the flow outside the wake. In the present case we take advantage of the derivation done by Nakayama,[5] which shows that when the shear layer is thin compared with the radius R, the pressure p is given by

$$p/\rho + \tfrac{1}{2}U_{\text{p}}^2 = p_{\text{ref}}/\rho + \tfrac{1}{2}U_{\text{ref}}^2 = \text{const.}, \tag{5}$$

where U_{p}, as mentioned earlier, is an extension of the external potential flow velocity into the wake and is obtained by joining the potential flow velocity distributions on the upper and lower sides of the

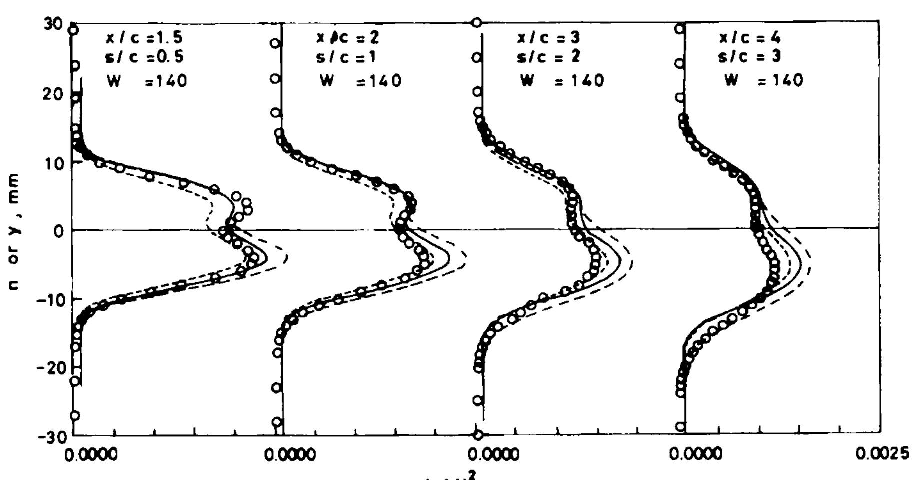

Figure 5(b). Profiles of turbulent kinetic energy, k/U_{ref}^2— Flow B; ○, experiment; ———, prediction with C_μ constant; — — —, prediction with C_μ variable (Leschziner and Rodi); --------, prediction with C_μ variable (Humphrey and Pourahmadi)

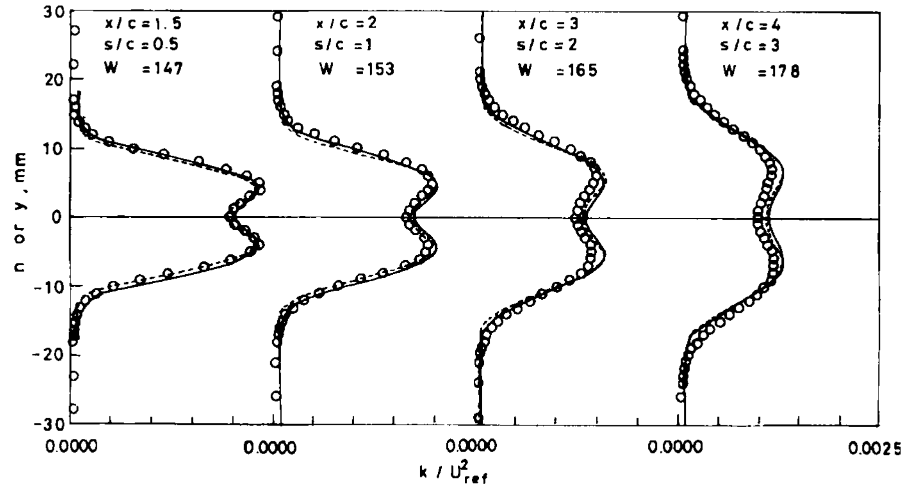

Figure 5(c). Profiles of turbulent kinetic energy, k/U^2_{ref}—Flow C: ○, experiment; ————, prediction with C_μ constant; — — —, prediction with C_μ variable (Leschziner and Rodi); ---------, prediction with C_μ variable (Humphrey and Pourahmadi)

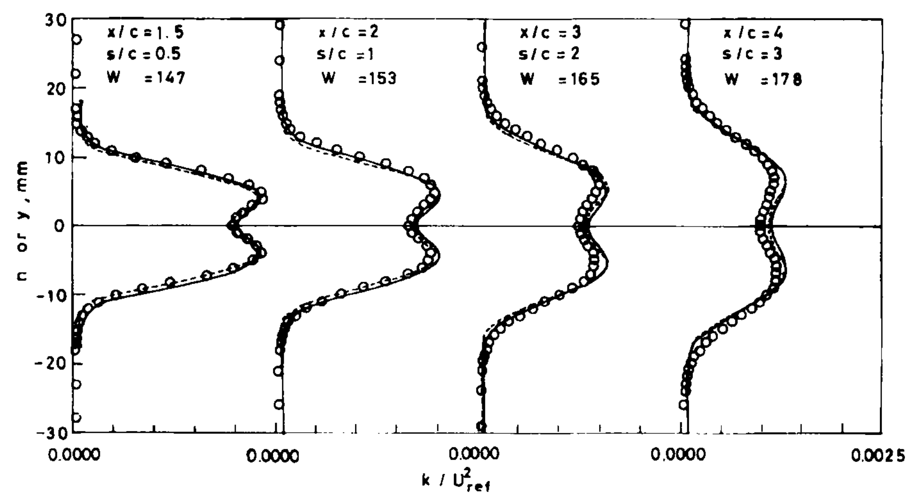

Figure 5(d). Profiles of turbulent kinetic energy, k/U^2_{ref}—Flow D: ○, experiment; ————, prediction with C_μ constant; ---------, prediction with C_μ variable (Humphrey and Pourahmadi)

wake. It was confirmed that the velocity distributions outside the wake are almost the same with and without the aerofoil and follow a straight line.[13] It was also confirmed that the static pressure at a point in the duct/diffuser was the same with or without the aerofoil.[13] Hence we use the experimental distribution of U_p in the curved duct/diffuser without the aerofoil and calculate $\partial p/\partial s$ using equation (5), i.e.

$$-(1/\rho)\partial p/\partial s = U_p \partial U_p/\partial s. \tag{6}$$

It may be remarked that So and Mellor[14] also used a similar procedure for analysing boundary layer data on curved surfaces. In the present investigation U_p can be expressed as

$$U_p = U_{pc}(s) - C(s)n, \tag{7}$$

where $U_{pc}(s)$ is the potential flow velocity at the centreline of the curved duct/diffuser and $C(s)$ is the slope of the straight line portion of the U_p versus n curve at a given location. In Flow B, U_{pc} was found to be a constant along the curved duct with a value of $1{\cdot}039\ U_{ref}$. However, in Flow C, U_{pc} varies with s and is represented by a cubic. The values of the slope $C(s)$ for Flows B and C were calculated from velocity profiles at the measuring stations without the aerofoil. A cubic polynomial was used to get a smooth fit to these values of $C(s)$.

After $\partial p/\partial s$ is known, a numerical solution to equations (2)–(4) is obtained by prescribing the profiles of U, k and ε at a suitable starting station and using the finite volume scheme of Patankar and Spalding.[15] The V-component of velocity is obtained by taking $V = 0$ at the duct/diffuser centreline and then integrating the continuity equation. Details of the discretization, the solution of the resulting equations, etc. are given in Reference 16. The initial profiles and the boundary conditions are treated in

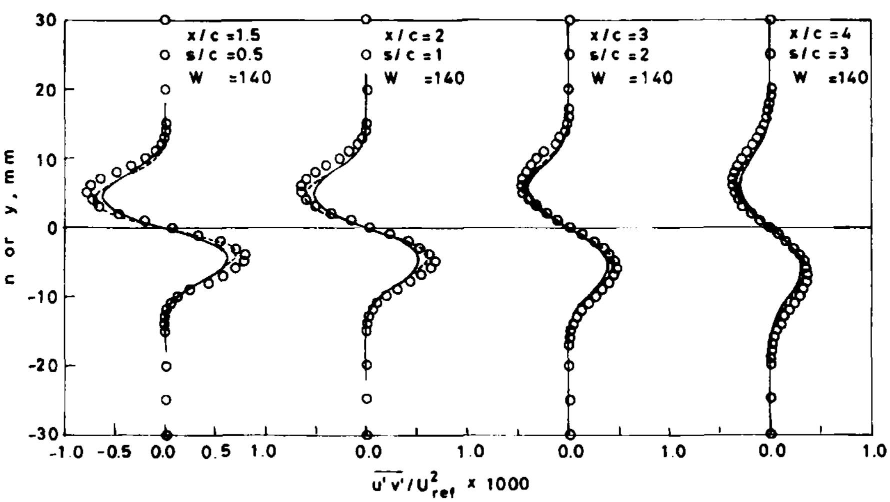

Figure 6(a). Profiles of Reynolds shear stress, $\overline{u'v'}/U^2_{ref}$—Flow A: ○, experiment; ———, prediction with C_μ constant; ---------, prediction with C_μ variable (Humphrey and Pourahmadi)

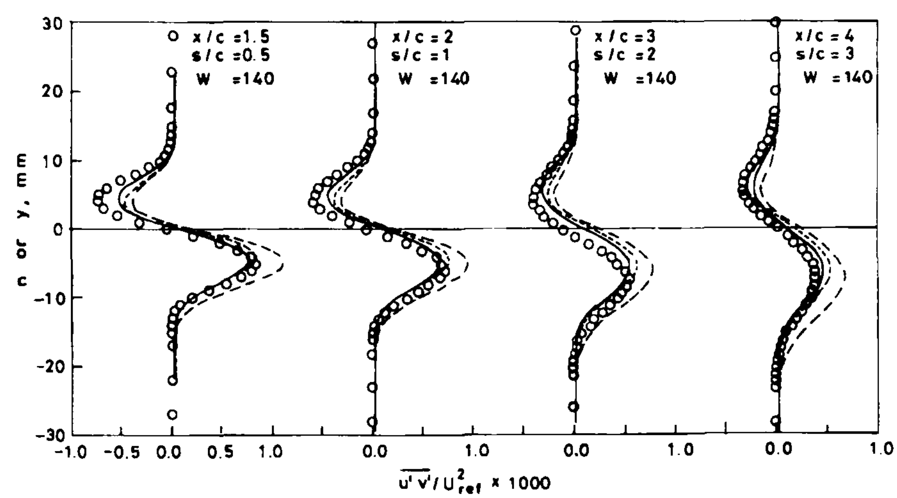

Figure 6(b). Profiles of Reynolds shear stress, $\overline{u'v'}/U^2_{ref}$—Flow B: ○, experiment; ———, prediction with C_μ constant; — — —, prediction with C_μ variable (Leschziner and Rodi); ---------, prediction with C_μ variable (Humphrey and Pourahmadi)

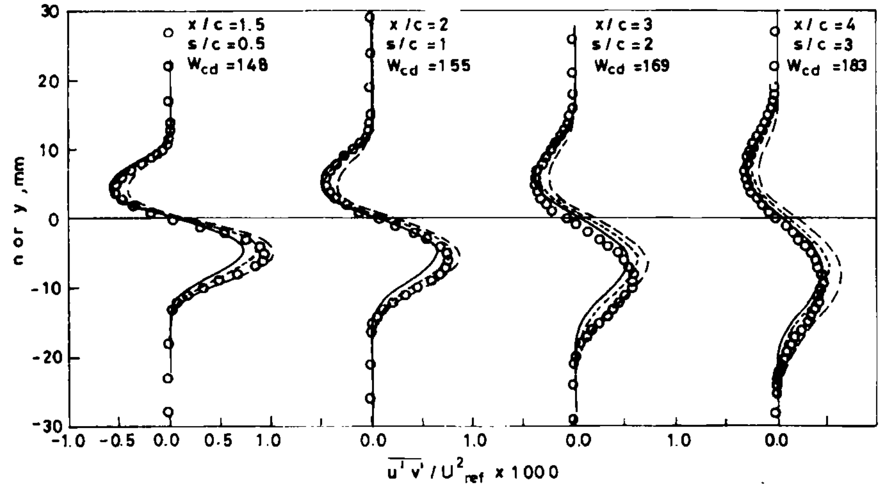

Figure 6(c). Profiles of Reynolds shear stress, $\overline{u'v'}/U_{\text{ref}}^2$—Flow C: ○, experiment; ————, prediction with C_μ constant; — — —, prediction with C_μ variable (Leschziner and Rodi); --------, prediction with C_μ variable (Humphrey and Pourahmadi)

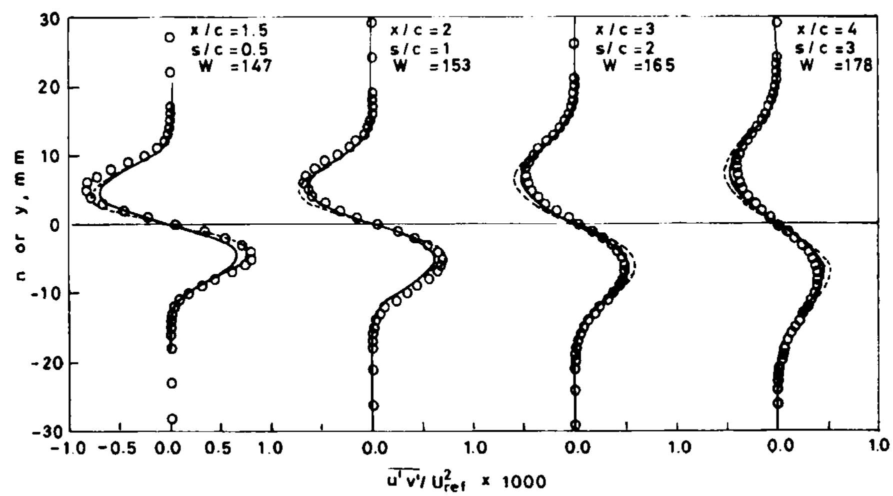

Figure 6(d). Profiles of Reynolds shear stress, $\overline{u'v'}/U_{\text{ref}}^2$—Flow D: ○, experiment; ————, prediction with C_μ constant; --------, prediction with C_μ variable (Humphrey and Pourahmadi)

a manner similar to that in Reference 8. A grid with 109 points across the wake, as prescribed by Badrinarayanan *et al.*,[11] is used and it gives grid-independent results.

4. RESULTS AND DISCUSSION

The computations were first carried out using the standard k–ε model. The full lines in Figures 2–6 represent the values obtained using the k–ε model with standard constants, described in the previous section. The following was observed. (i) For all cases the calculated velocity profiles are in close agreement with the experimental data (Figures 2(a)–2(d)). (ii) The values of W_0/U_p are slightly overpredicted (Figure 3) and those of b'_{avg} are slightly underpredicted (Figure 4). (iii) The calculated distributions of k and $\overline{u'v'}$ display the asymmetry in profiles due to the curvature in Flow B (Figures

5(b) and 6(b)). (iv) The enhancement in the asymmetric features of k and $\overline{u'v'}$ due to the additional presence of the adverse pressure gradient in Flow C is also displayed by the computations (Figures 5(c) and 6(c)). However, the computed values of the peaks in k are generally higher than the experimental values. The results for Flows A and D are in accordance with the fact that the k–ε model is satisfactory for the prediction of near and intermediate wakes in straight flows.[17,18] W_o/U_p and b'_{avg} also compare very closely with the experimental data in Flows A and D but are not shown for the sake of brevity.

In a recent lecture series, Leschziner[19] points out the known advantages and weaknesses of the standard k–ε model. The advantages that make it suitable for calculations of engineering accuracy are its ability to account for some of the physics of turbulence at moderate computational costs. Its weaknesses relate to its inadequate response to streamline curvature and adverse pressure gradient. He mentions a few suggestions to improve the performance of the k–ε model in these cases by modifying some of the model constants. Results of computations using these and other suggestions in the literature are given below.

Launder *et al.*[20] modify the constant $C_{\varepsilon 2}$ based on a curvature parameter. When this modification was tried out, it did not result in any significant improvement. This is perhaps because the expression for $C_{\varepsilon 2}$ in Reference 20 is based on a comparison with near-wall flows where the velocity gradient does not change sign.

Leschziner and Rodi[21] have considered the algebraic stress model and deduced by simplification that the k–ε model can be modified to account for the effect of curvature by making the model constant C_μ dependent on the local values of curvature, velocity gradient, k and ε. The proposed relationship is

$$C_\mu = \max\{0{\cdot}025, 0{\cdot}09/[1 + 0{\cdot}57(k^2/\varepsilon^2)(\partial U/\partial n + U/R)U/R]\}. \tag{8}$$

Computations with this modification are shown by long broken lines in Figures 2–6 for Flows B and C. It is seen that the agreement between the computed and experimental values of W_o/U_p and b'_{avg} is good. However, the peaks in k and $\overline{u'v'}$ show increased asymmetry as compared with those when the standard k–ε model is used. This leads to poorer agreement between the computed and experimental profiles of these quantities. It may be added that similar behaviour was seen by Narasimhan *et al.*[8] in the profiles of $\overline{u'v'}$ for which the comparisons were made.

Recently Tucker [22] has computed the flow behind the base of an axisymmetric body. In this case also the flow is subjected to curvature and pressure gradient effects. He has modified the k–ε model in the following manner. The model constant $C_{\varepsilon 1}$ is expressed as

$$C_{\varepsilon 1} = 1{\cdot}15 + 0{\cdot}25P_k/\varepsilon, \tag{9}$$

where P_k is the production of turbulent kinetic energy. The values of the other constants in the model are taken as $C_{\varepsilon 2} = 1{\cdot}90$, $\sigma_k = 0{\cdot}89$ and $\sigma_\varepsilon = 1{\cdot}15$. In the present case these modifications did improve the predictions of W_o/U_p and b'_{avg} as compared with those with the standard k–ε model, but the improvements in the profiles of k and $\overline{u'v'}$ were marginal.

Humphrey and Pourahmadi[23] (hereinafter referred to as H & P) and Pourahmadi and Humphrey[24] also start with the algebraic stress model and propose an expression for C_μ in the k–ε model. However, their approach differs from that of Leschziner and Rodi[21] in that the ratio of the production of turbulent kinetic energy to its rate of dissipation, i.e. P_k/ε, is not assumed to be unity. This leads to a more general expression for C_μ which can take into account the simultaneous effects of curvature and pressure strains in terms of (i) a curvature parameter δ which is the ratio of curvature strain to shear strain, i.e. $[U/(n+R)]/(\partial u/\partial n)$, and (ii) ratio P_k/ε. H & P give details of the derivation of the expression for C_μ. They have simplified the expression for C_μ and applied it to cases where the effects of curvature and P_k/ε can be separated, namely boundary layer, straight and curved channel flows. In the present case (Flow C) the effects of curvature and pressure gradient are combined. Hence, starting with the general expression of H & P an expression for C_μ was derived which depends on the curvature parameter δ and the ratio P_k/ε. The following expression is obtained:

$$C_\mu = \frac{\frac{2}{3}(1 - C_2)(1 - \delta)^2[C_1 - 1 + C_2(P_k/\varepsilon)] - 8(1 - C_2)^2\delta(1 + \delta)(P_k/\varepsilon)}{(1 - \delta)^2[C_1 - 1 + (P_k/\varepsilon)]^2}, \tag{10}$$

where C_1 and C_2 have values of 2·2 and 0·55 respectively as suggested by H & P. Results of the calculations using this modification are shown by short broken lines in Figures 2–6 for all four cases; in the case of Flows A and D the value of δ reduces to zero. The velocity profiles calculated using the H & P model and the standard k–ε model compare well with the experimental data (Figures 2(a)–2(d)) and the differences are not noticeable. The wake parameters W_0/U_p and b'_{avg} in Flows B and C show excellent comparison with the experimental values (Figures 3 and 4) when the H & P model is used. Further, the comparisons between the experimental and calculated peak values of k and $\overline{u'v'}$ show a significant improvement as compared with the standard k–ε model.

Thus, keeping in view the range of uncertainty in the experimental data, especially in k and $\overline{u'v'}$, it can be said that the k–ε model with modifications to C_μ, based on the curvature parameter and the ratio of the production of turbulent kinetic energy to its rate of dissipation, gives satisfactory results by being able to accommodate both curvature as well as mild adverse pressure gradient effects. The modified model gives an accurate prediction of the wake parameters W_0/U_p and b'_{avg}.

The following additional remarks can be made.

(i) Owing to the extremely low values of P_k/ε in a small region near the centre of the wake, equation (10) yielded unrealistically high values of C_μ and hence its value was limited to 0·15 in this region. The minimum value was limited to 0·025. H & P have set limits of $0{\cdot}045 \le C_\mu \le 0{\cdot}14$ in their calculations.

(ii) The H & P modification is also not entirely adequate to reproduce the experimental profiles of k and $\overline{u'v'}$ in curved flows. This is perhaps due to the fact that the modified expression for C_μ, though adequate over a significant portion of the wake, is not appropriate towards the edges of the wake. This was verified by plotting the values of C_μ using the far-wake data of Browne *et al.*[25] and by comparing them with the values of C_μ given by equation (10).

5. CONCLUSIONS

The development of wakes in a straight duct, a curved duct, a curved diffuser and a straight diffuser has been computed using thin shear flow equations and the k–ε model of turbulence. Calculations are performed with the model constant C_μ dependent on the curvature parameter and the ratio of the production of turbulent kinetic energy to its rate of dissipation, as suggested in Reference 23. The results are in good agreement with the experimental data and show that the scheme and modified k–ε model accurately predict the mean velocity profiles and wake parameters. Further, the scheme and model are adequate to capture the asymmetry in the profiles of the turbulent kinetic energy k and Reynolds shear stress $\overline{u'v'}$ caused by the curvature and its enhancement due to the additional presence of an adverse pressure gradient.

Though the scheme and model are adequate for calculations of engineering accuracy, the slight differences between the experimental and computed values of k and $\overline{u'v'}$ give rise to the view that a higher-order model, namely the Reynolds stress model, is perhaps required for better prediction of k and $\overline{u'v'}$.

ACKNOWLEDGEMENT

The computations were carried out on an IBM-PC-AT 486 bought for an ISRO-funded project on 'Computations of supersonic turbulent base flows'. The support from the funding agency is gratefully acknowledged.

REFERENCES

1. R. Chevray and L. S. G. Kovasznay, 'Turbulence measurements in the wake of a flat plate', *AIAA J.*, **6**, 1641–1643 (1969).
2. P. J. Pot, 'Measurements in a 2-d wake and in a 2-d wake merging into a boundary layer', *Data rep. NLR TR-79063 U*, 1979.
3. P. E. Lemonnier, J. H. Garem and L. F. Tsen, 'Sillage turbulent cree par une plaque plane en acoulement fortement decelere', *Contrat DRME 73.765, 2e Rapport Semestriel*, Centre D'etudes Aerodynamiques et Thermiques, 1974.
4. A. M. Savil, 'The turbulence structure of a highly curved two-dimensional wake', in R. Dumas and F. Fulachier (eds), *IUTAM Symp. on Complex Turbulent Flows*, Springer, Berlin, 1983, pp. 185–197.
5. A. Nakayama, 'Curvature and pressure-gradient effects on a small defect wake', *J. Fluid Mech.*, **175**, 215–246 (1987).
6. V. Ramjee, E. G. Tulapurkara and R. Rajasekar, 'Development of airfoil wake in a longitudinally curved stream', *AIAA J.*, **26**, 948–953 (1988).
7. V. Ramjee and D. Neelakandan, 'Curvature effects on the wake of an airfoil and other bodies', *Fluid Dyn. Res.*, **6**, 1–13 (1990).
8. J. L. Narasimhan, V. Ramjee, P. M. Diwakar and E. G. Tulapurkara, 'Prediction of wake in a curved duct', *Int. j. numer. methods fluids*, **13**, 907–916 (1991).
9. E. G. Tulapurkara, V. Ramjee and J. George, 'Development of wake in presence of both curvature and pressure gradient', *Proc. Symp. on Boundary Layer and Free Sher Flows*, ASME, New York, 1994, pp. 195–202.
10. R. W. Fox and S. J. Kline, 'Flow regimes in curved subsonic diffusers', *Trans. ASME, J. Basic Eng.*, **84**, 303–312 (1962).
11. M. A. Badrinarayanan, S. Raghu and E. G. Tulapurkara, 'The non-equilibrium region of a mixing layer', *AIAA J.*, **23**, 987–991 (1985).
12. W. Rodi and G. Scheuerer, 'Calculation of curved shear layers with two equation turbulence models', *Phys. Fluids*, **26**, 1422–1436 (1983).
13. J. George, 'Development of wakes under the combined influence of curvature and pressure gradient', *M.S. Thesis*, Department of Aerospace Engineering, Indian Institute of Technology, Madras, 1994.
14. R. M. C. So and G. L. Mellor, 'Experiment on convex curvature effects in turbulent boundary layers', *J. Fluid Mech.*, **60**, 43–62 (1973).
15. S. V. Patankar and D. B. Spalding, 'A finite difference procedure for solving the equation of two dimensional boundary layer', *Int. J. Heat Mass Transfer*, **10**, 1389–1411 (1967).
16. E. G. Tulapurkara and J. L. Narasimhan, 'Numerical scheme to compute development of wake in a curved stream', *Rep. AE-TR-90-1*, Department of Aerospace Engineering, Indian Institute of Technology, Madras, 1990.
17. E. G. Tulapurkara, S. Vengadesan and J. L. Narasimhan, 'Calculation of laminar and turbulent asymmetric wakes', in C. Taylor, J. H. Chin and G. M. Homsy (eds), *Numerical Methods in Laminar and Turbulent Flows*, Vol. VII, Pineridge, Swansea, 1991, pp. 337–347.
18. V. C. Patel and G. Scheuerer, 'Calculation of two-dimensional near and far wake', *AIAA J.*, **20**, 900–907 (1982).
19. M. A. Leschziner, 'Two-equation models for high Reynolds-number flow', in *Introduction to the Modelling of Turbulence*, Lecture Series 1993-02, von Karman Institute for Fluid Dynamics, 1993, pp. TM2–TM41.
20. B. E. Launder, C. H. Priddin and B. I. Sharma, 'The calculation of turbulent boundary layers on spinning and curved surfaces', *ASME J. Fluids Eng.*, **99**, 231–239 (1977).
21. M. A. Leschziner and W. Rodi, 'Calculations of annular and twin parallel jets using various discretization schemes and turbulence-model variations', *ASME J. Fluids Eng.*, **103**, 352–360 (1981).
22. P. K. Tucker, 'Validation of a computational fluid dynamics (CFD) code for supersonic axisymmetric base flow', *NASA CP 3221*, part 1, 1993.
23. J. A. C. Humphrey and F. Pourahmadi, 'A generalised algebraic relation for predicting developing curved channel flow with a k–ε model of turbulence', *LBL Rep. 12009 Rev.*, University of California at Berkeley, 1981.
24. F. Pourahmadi and J. A. C. Humphrey, 'Prediction of curved channel flow with an extended k–ε model of turbulence', *AIAA J.*, **21**, 1365–1373 (1983).
25. L. W. B. Browne, R. A. Antonia and D. A. Shah, 'Turbulent energy dissipation in a wake', *J. Fluid Mech.*, **179**, 307–326 (1987).